

# **Smart Manufacturing and Material Processing** (SMMP)

DOI: http://doi.org/10.26480/smmp.01.2023.66.71





#### REVIEW ARTICLE

### DESIGN AND OPTIMIZATION OF MECHANICAL STRUCTURES FOR WALL-CLIMBING ROBOTS

Ling Chena, Rongjuan Suia, Yuzhu Zhengb, Xinjian Chena, Xuanben Xiec, Muhammad Zeeshan Zahird

- <sup>a</sup>School of Engineering Machinery, Shandong Jiaotong University, Jinan, China
- bhalma Group Corporation, Weifang, China
- <sup>c</sup>The Development Service Center of Jimo Ancient City, Qingdao, China
- <sup>d</sup>Mechanical Engineering Department, University of Engineering & Technology, Peshawar, Pakistan
- \*Corresponding Author Email: srj\_pp@163.com

This is an open access article distributed under the Creative Commons Attribution License CC BY 4.0, which permits unrestricted use, distribution, and reproduction in any medium, provided the original work is properly cited.

#### **ARTICLE DETAILS**

#### Article History:

Received 05 January 2024 Revised 08 February 2024 Accepted 11 March 2024 Available online 14 March 2024

#### **ABSTRACT**

There is a problem of insufficient adsorption capacity of the wall-climbing robot on the steel wall during its movement. The paper designs a magnetically adsorbed wall-climbing robot with triangular track wheels, which includes a walking structure, a drive structure, and a magnetically adsorbed structure. Firstly, the robot was designed using 3D mapping software to determine a triangular crawler wheel travel and permanent magnet adsorption solution. The mechanical model of the wall climbing robot on a steel wall is then analyzed statically to obtain the minimum adsorption force to be adsorbed on the steel wall. Finally, the magnet structure is analyzed by ANSYS magnetic simulation software to optimize the structure of the permanent magnet and design the most suitable height of the magnetic track wheel, providing a reference for the design and optimization of the permanent magnet adsorption structure of the wall climbing robot.

#### KEYWORDS

Wall-climbing robots, static analysis, emulation, optimize the design

#### 1. Introduction

In recent years, wall climbing robots have been used in steel wall inspection, glass curtain wall cleaning, and other applications (Lei et al., 2023; Shigenori et al., 2021; Weiping, 2005). Depending on the adsorption mode, the adsorption methods can be grouped into the following categories: magnetic adsorption, vacuum adsorption, adhesion material adsorption, and reaction force adsorption (Xianyu and Hualun, 2018). For steel walls, permanent magnetic adsorption has unique advantages over other modes in terms of adsorption force, load capacity, and wall adaptability, so permanent magnetic adsorption is used the most for wall-climbing robots (Peihan et al., 2022).

Pan Huanhuan et al developed a boiler water-cooled wall cleaning and inspection wall climbing robot, whose adsorption function was achieved using double tracks, 30 permanent magnetic adsorption blocks were installed on each track, of which at least 5 blocks on each track were in good contact with the wall surface, thus enabling the robot to adhere to the wall surface (Huanhuan et al., 2000). The disadvantage of this robot is the large size of the structure and the tendency to fall off when walking on the transition wall. Wang Mingqiang et al designed a new multi-tracked omnidirectional Wall climbing robot (Wang et al., 2021). The multi-tracked omnidirectional wall-crawling robot was able to travel freely on the wall, abandoning the traditional track differential steering method and avoiding the tendency to turn during robot motion, but the small contact area between the permanent magnet and the wall led to poor adsorption and weak load capacity. Song Wei et al developed a magnetic adsorption wallcrawler robot, which improved the magnetic mass ratio and load capacity of the wheeled wall-crawler robot by optimizing the magnetic adsorption component (Wei et al., 2018). However, the machine is currently deficient in barrier-crossing capability. Jiang Aimin et al developed a two-joint wheeled robot with wall transition capability to cross large obstacles on

the wall, but its control is difficult to achieve the control stability performance required in the industry (Aimin et al., 2018). The strength of the adsorption performance of permanent magnet wall-climbing robots is closely related to the development of wall-climbing robots.

In this study, a magnetic triangular crawler wheel wall-crawler robot was developed, and its adsorption structure was simulated and optimized using ANSYS software to find a better solution to the problem of detection due to insufficient adsorption force.

#### 2. OVERALL STRUCTURAL DESIGN OF THE CLIMBING ROBOT

The three-dimensional structure of the wall-crawler robot is shown in Figure 1. The robot is composed of an adsorption structure, a transmission structure, a drive structure, and a detection structure. The drive structure and the detection device are installed in the vehicle box. The adsorption structure is installed inside the robot's track wheels, which are in direct contact with the wall surface to ensure that the wall-crawler can adsorb to the wall surface more stably. The track wheels are connected to the vehicle frame through the inner and outer ball cage structure so that they can rotate within a certain range and have a certain wall transition capability.

#### 2.1 Permanent Magnetic Adsorption Design

The permanent magnet adsorption structure of the wall climbing robot consists of four triangular track wheels, mounted at the corners of the vehicle. Each magnetic triangular track wheel consists of drive gears Q1, Q2, Q3 drive wheel Q4, track, and wheel carrier, as shown in Figure 2. For the robot crawling steadily on the wall, the permanent magnets are fixed to the outer tracks and in contact with the wall surface.

Each track has 33 permanent magnet adsorption units, one permanent magnet for each permanent magnet adsorption unit, which is connected by the tracks. The sizes of the magnet are  $30 \text{ mm} \times 8 \text{ mm} \times 8 \text{ mm}$ .

Quick Response Code

Access this article online

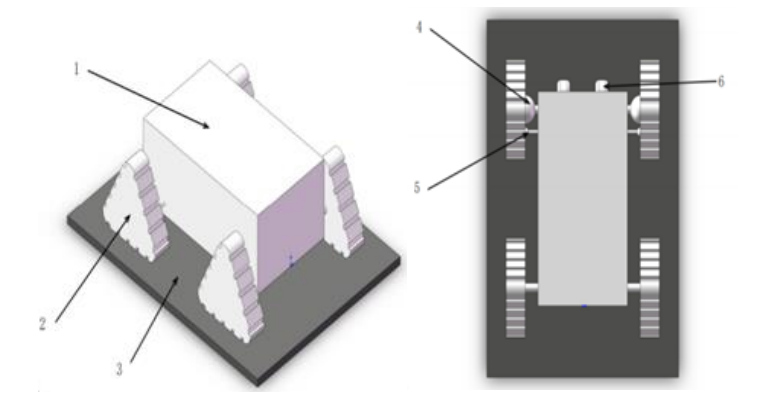
DOI:

10.26480/smmp.01.2023.66.71

**Website:**Website: www.topicsonchemeng.org.my

As shown in Figure 3, the track wheel frame acts as the overall support structure. The shaft where the drive gear is located is fixed to the track wheel frame, the drive gear and drive wheel are in a stacked design, and

the three layers of the structure can be taken off the shaft of the drive gear in turn, and each gear and shaft contact position is fixed by a key to improving the stability of the internal drive structure.



1 - Body; 2 - Triangular track wheels; 3 - Wall; 4 - Steering ball cage; 5 - Steering lever; 6 - Detection device

Figure 1: 3D structural model of the robot

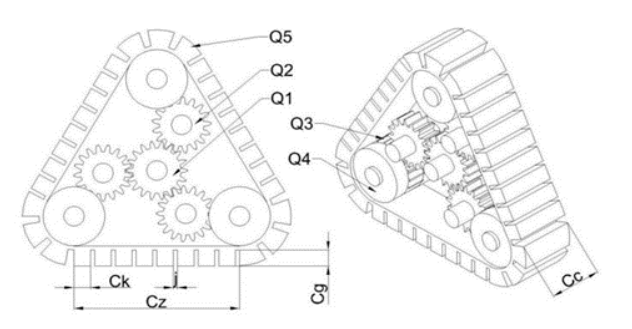
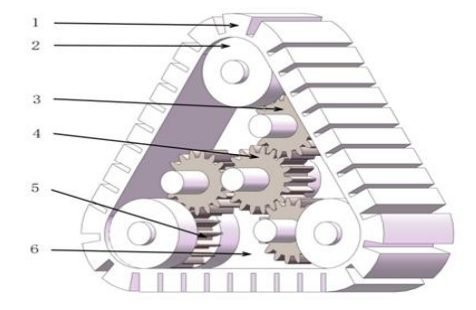


Figure 2: Triangular track wheel structure



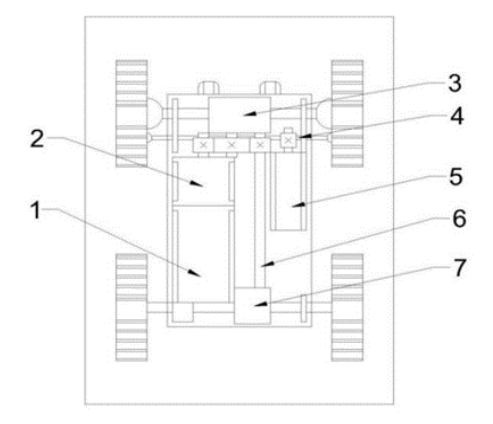
1 - magnetic track; 2 - drive wheel; 3 - drive gear; 4 - centre gear; 5 - drive gear; 6 - track wheel frame

Figure 3: 3D structural model of the magnetic triangular track wheel

#### 2.2 Design of the Drive Structure

The movement of the wall climbing robot is driven by a drive motor, which is mounted in the vehicle box. Inside the vehicle box, a planetary reducer transmits the decelerated power through gears to the drive shaft, which is traditionally connected to the front and rear differentials to achieve

turning activities on the wall (Nakamura, 1993). The output shaft gear of the steering motor is directly connected to the steering rod, which is fixed with a rack and pinion, which transmits the power from the motor to the steering rod with the cooperation of the rack and pinion. As shown in Figure 4.



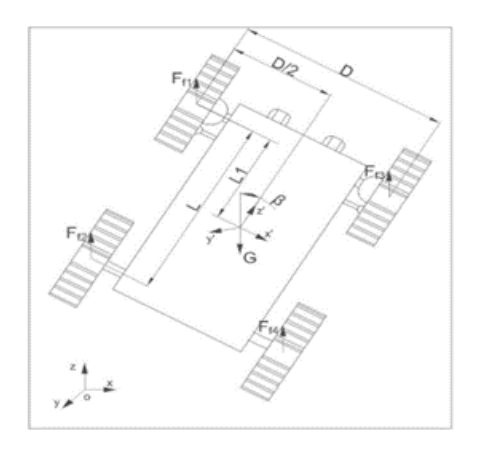
1 - drive motor; 2 - planetary gearbox; 3 - front differential; 4 - rack and pinion steering rod; 5 - steering motor; 6 - drive shaft; 7 - rear differential

Figure 4: Diagram of the transmission method

#### 3. Analysis of REliable Adsorption Conditions for Wall-Climbing Robots

The three main forms of instability caused by this robot when the wall-crawling robot is statically attached to a large metal wall are as follows: (1) The robot tends to slide along the wall. (2) The robot tends to tip longitudinally (Liu et al., 2022). (3) The robot tends to tilt laterally. In these cases, there is a risk of the wall climbing robot breaking away from the wall in the case of static adsorption, so the following scenarios are investigated for this robot.

The forces applied to the wall climbing robot in different attitudes and positions are shown in Figure 5.  $\beta$  is the attitude angle of the robot and is the angle between the z-axis and the z'-axis, taking values in the range  $[0^{\circ},360^{\circ}]$ , and G is the overall gravitational force of the wall-climbing robot at maximum load.  $F_{\rm fi}$  is the friction force on the individual track wheels,  $F_{\rm zi}$  is the support force on the individual track wheels and  $F_{\rm xi}$  is the adsorption force on the individual track wheels. The four-track wheels are of the same design, so  $F_{\rm xi}=F_{\rm x}$  and  $\mu$  is the friction between the metal wall and the magnet, taking  $\mu$ =0.5.



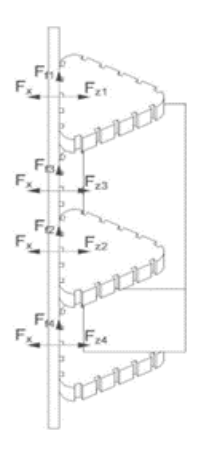


Figure 5: Force analysis of the wall surface of the wall climbing robot

#### 3.1 Slip Analysis on Wall Surfaces

Wall climbing robots tend to slide along the wall. For the robot to be stationary on the wall, the friction between the robot and the wall should be greater than the sum of the external forces along the wall.

The force equation for the wall-climbing robot on the wall is as follows:

$$\begin{cases} \sum_{i=1} F_{FI} \ge G \\ F_{fi} = \mu \cdot F_{zi} \end{cases}$$

$$\sum_{i=1}^{4} F_{xi} = \sum_{i=1}^{4} F_{zi}$$

$$(1)$$

Collated from:

$$F_X \ge \frac{G}{4\mu} \tag{2}$$

#### 3.2 Overturning Analysis on Walls

The tilting forces on the wall climbing robot, as it moves in any direction ( $\beta \in [0,360]$ ) on the wall, are analyzed and the forces on the vertical wall for the wall climbing robot are shown in Figure 5. As the wall climbing robot moves on the wall, the support forces on the four of the triangular track wheels change as the  $\beta$  angle changes, so the adsorption forces on the triangular track wheels have to be calculated to ensure that they can be used in different attitudes to ensure that the robot does not break away from the wall under tipping forces.

$$\begin{cases} F_{Z1} = F_{X1} - \frac{\cos \beta \cdot G \cdot S}{2L} - \frac{\sin \beta \cdot G \cdot S}{2D} \\ F_{Z2} = F_{X2} + \frac{\cos \beta \cdot G \cdot S}{2L} - \frac{\sin \beta \cdot G \cdot S}{2D} \\ F_{Z3} = F_{X3} - \frac{\cos \beta \cdot G \cdot S}{2L} + \frac{\sin \beta \cdot G \cdot S}{2D} \\ F_{Z4} = F_{X4} + \frac{\cos \beta \cdot G \cdot S}{2L} + \frac{\sin \beta \cdot G \cdot S}{2D} \\ F_{X} = F_{X1} = F_{X2} = F_{X3} = F_{X4} \end{cases}$$
(3)

During the robot's motion, no tipping will occur as long as the support force  $F_{zi} > 0$  for each of the triangular track wheels, so the collation gives:

$$\begin{cases} F_{x1} > \frac{G \cdot S}{2} \left( \frac{\sin \beta}{D} + \frac{\cos \beta}{L} \right) \\ F_{x2} > \frac{G \cdot S}{2} \left( \frac{\sin \beta}{D} - \frac{\cos \beta}{L} \right) \\ F_{x3} > \frac{G \cdot S}{2} \left( -\frac{\sin \beta}{D} + \frac{\cos \beta}{L} \right) \\ F_{x4} > \frac{G \cdot S}{2} \left( -\frac{\sin \beta}{D} - \frac{\cos \beta}{L} \right) \end{cases}$$

$$(4)$$

It can be seen that when  $F_x \ge F_{xi}$ , the wall climbing robot will not peel over on any of the track wheels, where S is the distance of the center of gravity from the plane of contact.

#### 3.3 Robot Adsorption State Extremum Calculation

Based on the common instability states of wall-climbing robots above, the maximum adsorption force required for a wall-climbing robot is

$$F_{\partial} \ge K \cdot \max \left\{ \left\{ \frac{G}{4\mu}, \frac{GS}{2} \left( \frac{\sin \beta}{D} + \frac{\cos \beta}{L} \right) \right\}$$
 (5)

Where K is the safety factor. According to the design parameters can be obtained: G = 200N, H = 48mm, L = 420mm,  $\mu = 0.5$ , K = 1.5, S = 290mm. will be substituted into the various parameters of the formula (6) can be obtained:  $F_m \ge 100$ N.

From the calculations, it is clear that to achieve safe adsorption for this robot, the adsorption force  $F_m \ge 100$  N needs to be provided by each track wheel of the adsorption that fits against the wall.

# 4. FINITE ELEMENT SIMULATION ANALYSIS OG MAGNETIC ADSORPTION DEVICES

#### 4.1 Basic Magnetic Field Theory

The magnetic field of the magnetic triangular crawler wheel of the wall climbing robot is a static magnetic field, the distribution of which is by Maxwell's electromagnetic theory. To simplify the magnetic field solution, the vector magnetic potential *A* is introduced:

$$\overrightarrow{B} = \nabla \times \overrightarrow{A} \tag{6}$$

Where *B* is the magnetic induction intensity.

Based on the Maxwell system of equations, the dielectric intrinsic relations, and the Coulomb norm, it can be deduced that

$$\nabla \times \left(\frac{1}{\mu} \nabla \times \overrightarrow{A}\right) = \overrightarrow{J} \tag{7}$$

where  $\mu$  is the magnetic permeability of air and J is the conduction current density.

Combining equation (6) and expanding (7) in the coordinate system yields

$$\begin{cases} \frac{\partial}{\partial y} \left(\frac{1}{\mu}\right) \left(\frac{\partial Ay}{\partial x} - \frac{\partial Ax}{\partial y}\right) - \frac{\partial}{\partial z} \left(\frac{1}{\mu}\right) \left(\frac{\partial Ax}{\partial z} - \frac{\partial Az}{\partial x}\right) - \frac{1}{\mu} \left(\nabla^{2} \overrightarrow{A}\right)_{x} = J_{x} \\ \frac{\partial}{\partial z} \left(\frac{1}{\mu}\right) \left(\frac{\partial Ay}{\partial y} - \frac{\partial Ax}{\partial z}\right) - \frac{\partial}{\partial z} \left(\frac{1}{\mu}\right) \left(\frac{\partial Ay}{\partial x} - \frac{\partial Ax}{\partial y}\right) - \frac{1}{\mu} \left(\nabla^{2} \overrightarrow{A}\right)_{y} = J_{y} \\ \frac{\partial}{\partial x} \left(\frac{1}{\mu}\right) \left(\frac{\partial Ax}{\partial z} - \frac{\partial Az}{\partial x}\right) - \frac{\partial}{\partial y} \left(\frac{1}{\mu}\right) \left(\frac{\partial Az}{\partial y} - \frac{\partial Ay}{\partial z}\right) - \frac{1}{\mu} \left(\nabla^{2} \overrightarrow{A}\right)_{z} = J_{z} \end{cases}$$
(8)

where:

$$\left(\nabla^{2} \overrightarrow{A}\right)_{x} = \frac{\partial^{2} A x}{\partial x^{2}} + \frac{\partial^{2} A x}{\partial y^{2}} + \frac{\partial^{2} A x}{\partial z^{2}} \\
\left(\nabla^{2} \overrightarrow{A}\right)_{x} = \frac{\partial^{2} A y}{\partial x^{2}} + \frac{\partial^{2} A y}{\partial y^{2}} + \frac{\partial^{2} A y}{\partial z^{2}} \\
\left(\nabla^{2} \overrightarrow{A}\right)_{x} = \frac{\partial^{2} A z}{\partial x^{2}} + \frac{\partial^{2} A z}{\partial y^{2}} + \frac{\partial^{2} A z}{\partial z^{2}}$$

$$(9)$$

Where,  $A_x$ ,  $A_y$ ,  $A_z$ ,  $B_x$ ,  $B_y$ ,  $B_z$ ,  $J_x$ ,  $J_y$ , and  $J_z$  are the components of A, B, and J in the x, y, and z directions in the three-dimensional coordinate system. Combined with the actual magnetic circuit structure and boundary conditions, a unique solution for the magnetic field parameters can be found. The adsorption force is also an important indicator in magnetic field analysis and can be calculated between the permanent magnet wheel and the wall of the steel structure using the Maxwell tension method as follows:

$$\oint_{S} T dS = \oint_{S} \left[ \frac{1}{\mu} \begin{pmatrix} \overrightarrow{B} \cdot \overrightarrow{n} \end{pmatrix} - \frac{1}{2\mu} \begin{pmatrix} \overrightarrow{B}^{2} \cdot \overrightarrow{n} \end{pmatrix} \right] dS$$
(10)

Where: S is the closed surface of the medium enclosing the magnetic field, n is the unit vector in the direction normal to the outside of ds, B is the magnetic induction intensity on the closed surface and u is the magnetic permeability of the air.

The above static magnetic field model is the fundamental basis for finite element simulation. From equation (10), it can be seen that the permanent magnet adsorption structure model must be enclosed in the air when solving for the adsorption force using ANSYS software.

## 4.2 Simulation Analysis and Structural Optimization of Magnetic Delta Track Wheels

#### 4.2.1 Defining Materials

Magnets made of permanent magnetic materials, once magnetized, remain magnetic for a long time. A comparison of the performance parameters of various common magnetic materials shows that NdFeB has the advantage of higher remanence, higher coercivity, and higher magnetic energy product than other magnetic materials, and also has better mechanical properties. The NdFeB grade N35 was chosen as the material for the permanent magnets of the triangular track wheel and its magnetic properties are shown in Table 1:

Table 1: N35 Magnet Performance Parameters	
Performance parameters	Numerical values
Residual magnetism(T)	1.17-1.21
orthopaedic force (KA/m)	≥868
endowed with orthopedic powers (KA/m)	≥955
Maximum magnetic energy product $(KJ/m^3)$	263-287
Maximum working temperature (°C)	80

# 4.2.2 Simulation and Analysis of The Magnetic Field of The Magnetic Delta Track Wheel

The magnet material on the track of the magnetic triangular track wheel has been determined to be NdFe35, and its parametric properties have been specified. The material chosen for the walls is ordinary structural steel, and the medium in the space where the wheel is located in air.

For the design of the geometrical parameters, all actual parameters were used to simulate the actual situation accurately. The initial distance between the permanent magnets and the tank wall was set at 1mm for consideration of the permeability of the steel wall coating and the plating, where the permanent magnet material is NdFe35, the steel wall material is high-quality carbon steel, the air gap is air and the relative permeability is  $\mu$ =1.0. triangular track wheels are the same structure, so only a single magnetic triangular track wheel is simulated in this simulation analysis.

Due to the large size of the 3D model, the 3D magnetic field is extremely computationally intensive to analyze, so the model meshes before the analysis is carried out, setting the minimum mesh length to 6mm and turning on adaptive adjustment within a certain range. After meshing, the solution is started by adding flux parallel boundary conditions to the air calculation domain and adding flux intensity and flux density solution parameters to all models as a whole, with the total magnetic flux and total magnetic induction intensity shown in Figure 6 and Figure 7.

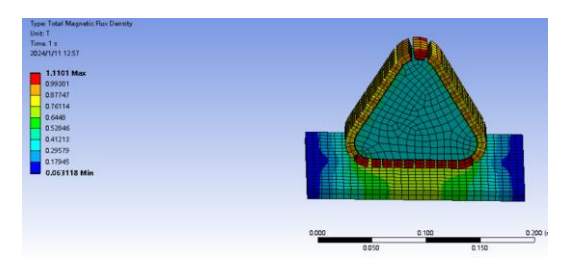


Figure 6: Total magnetic flux density

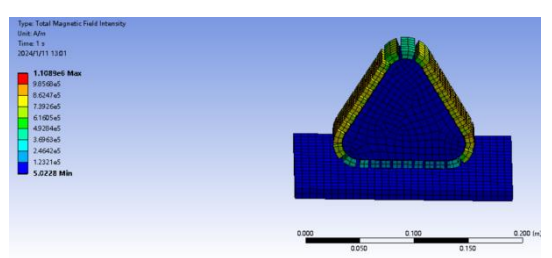


Figure 7: Total magnetic field intensity

Figure 6 and Figure 7 show the distribution of magnetic force and suction, with greater magnetic force on both sides and less suction in the middle. This is because the track wheel frame is made of metal and will form an integrated guide to the magnetic force of multiple magnets, creating a phenomenon where the magnetic force is greater at the bend on both sides and less at the smooth middle.

#### 4.2.3 Structural Optimization of Magnetic Triangular Track Wheels

The guideline for the optimal design of permanent magnet structures is to maximize the utilization of magnetic energy (Zheng rt al., 2021). The optimized design solution is proposed while satisfying the adsorption conditions of the wall climbing robot. In this paper, a control variable

approach is used to select the height of different magnetic triangular track wheels for analysis using ANSYS.

The design of the triangular track pulley requires the selection of a suitable pulley height to maximize the use of the adsorption force. With the permanent magnet pulley dimensions unchanged, the height of the

triangular track pulley is set to 4, 6, 8, and 10mm respectively. A static magnetic field simulation of the triangular track pulley is carried out and after solving for the magnetic triangular track pulley, the total magnetic flux density, total magnetic field strength, combined force, and the adsorption force in the Y-axis direction can be visualized. As shown in Figure 8.

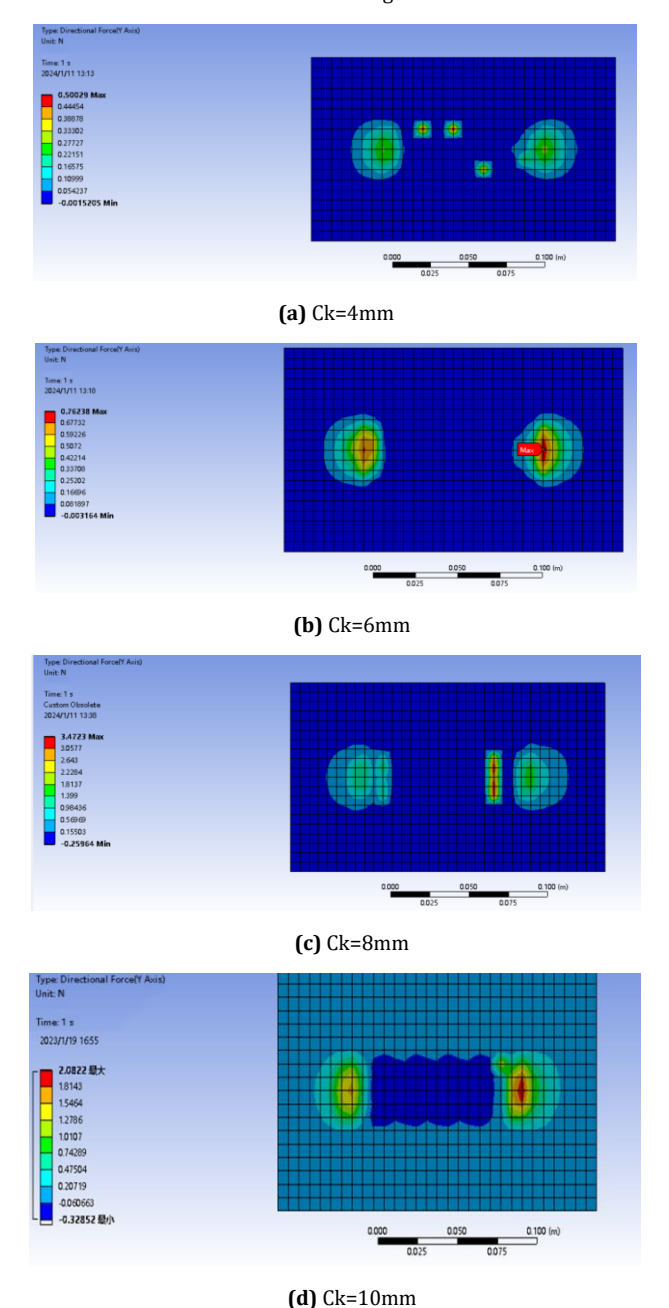


Figure 8: Adsorption forces for different magnetic triangular track wheel heights

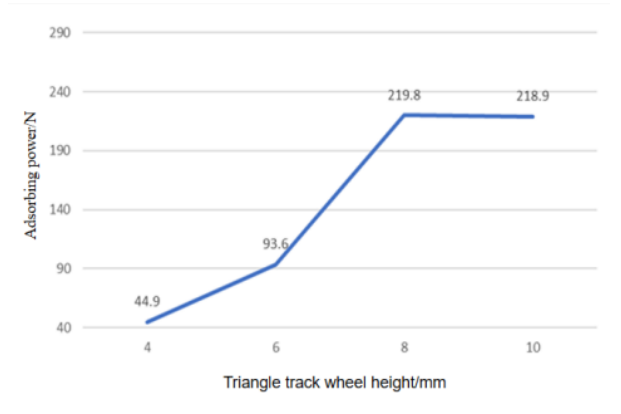


Figure 9: Effect of the height of the triangular track wheel on the adsorption force

From Figure 9, it can be concluded that the adsorption force of the permanent magnet wheel is proportional to the height of the track wheel,

with the rest of the conditions being the same, but the magnetic triangular track wheel does not meet the adsorption requirements of the robot at

heights of 4mm and 6mm. After a height of 8 mm, the rate of increase slows down and reaches a critical saturation point, as shown in Figure 10. At this point, the adsorption force has met the overall robot design requirements, a minimum adsorption force of 100N is achieved and the wall-crawler can adsorb and crawl normally on the wall surface. Considering that the wall crawler was as lightweight as possible and cost-effective as possible in meeting the adsorption conditions, the track wheel height was chosen to be 8mm.

#### 5. CONCLUSION

In this study, the magnetic triangular crawler wheel wall climbing robot was designed. The adsorption structure and transmission structure were designed, and the adsorption force learned by the robot in wall adsorption was calculated The magnetic adsorption structure was simulated and the structural parameters were optimized.

A static analysis of the robot in the working condition on the wall was carried out and the minimum adsorption force required to be provided by a single magnet was calculated from the instability form analysis.

Optimisation of the triangular track pulley. On the premise that the overall structural dimensions of the permanent magnet remain unchanged, the thickness of the magnetic triangular track pulley is optimized to make the pulley as light as possible, and the thickness of the different magnetic triangular track pulleys is simulated by ANSYS to obtain a better track pulley thickness while satisfying the minimum adsorption force is 100N.

#### **ACKNOWLEDGMENT**

Acknowledgement of the support from Shandong Jiaotong Institute of Science and Technology Innovation Project 2023YK049, Mechanical structure design of tank wall climbing robot; 2023YK058, Research and development of ultrasonic rolling surface strengthening device for the inner surface of large tanks.

#### REFERENCES

Aimin, J., Qiang, Z., Yin, Z., 2018. Development of a new magnetic adsorption wall climbing robot. Machine Manufacturing and Automation, 47 (4), Pp. 146-148 + 161.

- Huanhuan, P., Yanzheng, Z., Shuliang, L., 2000. Attitude control of a multifunctional tracked magneto-absorbent wall-climbing robot. Journal of Harbin Institute of Technology, (02), Pp. 5-8+11.
- Lei, L., Xing, Y., Xujie, Q., Yaqian, W., 2023. Research status and development trend of wall climbing and cleaning robots. Machine Manufacturing and Automation, 52 (01), Pp. 1-6.
- Liu, J.F., Hong, X.W., Chen, Y., Nie, Y.C., 2022. Optimized design of permanent magnet wheel for large steel structure inspection wall climbing robot. Manufacturing Automation, 44 (01), Pp. 46-50.
- Nakamura, S.,1993. Applied Numerical Methods in C. 3rd. USA: Prentice-Hall International.
- Peihan, N., Yating, Z., Yong, C., 2022. A review of wall climbing robot development and key technologies. Machine Tools and Hydraulics, 50 (04), Pp. 155-161.
- Shigenori, S., Daisuke, T., Atsunori, I., Teruhiro, I., 2021. Image Mosaicking and Localization Using a Camera Mounted on a Hanging-Type Wall Climbing Robot. irobomech, 33 (6).
- Wang, M.Q., Chen, J., Fang, H.F., 2021. Structural design of a new multitracked omnidirectional wall climbing robot. Mechanical Design and Manufacture, (05), Pp. 208-211+216.
- Wei, S., Hongjian, J., Tao, W., 2018. Optimal design and experimental study of magnetic adsorption assembly for wall climbing robot. Journal of Zhejiang University (Engineering Edition), 52 (10), Pp. 1837-1844.
- Weiping, Z., 2005. Inspection and repair methods for common defects in oil storage tanks. Journal of Petroleum and Natural Gas, (S4), Pp. 186-188.
- Xianyu, M., Hualun, D., 2018. Structural design of wall climbing robot and research on key technology of curved magnetic adsorption. Manufacturing Automation, 40 (06), Pp. 19-22+39.
- Zheng, Y.F., Liu, H.X., 2021. Design and analysis of an adaptive wheel-andfoot wall-climbing robot. Mechanical Design, 3 8 (09), Pp. 105-112.

